Sensors and Actuators B 162 (2012) 184–193

Contents lists available at SciVerse ScienceDirect

Sensors and Actuators B: Chemical

journal homepage: www.elsevier.com/locate/snb

Development of a flexural plate-wave (FPW) immunoglobulin-E (IgE) allergy bio-sensing microsystem

I.-Y. Huang, M.-C. Lee, C.-H. Hsu, C.-C. Wang*

Department of Electrical Engineering, National Sun Yat-sen University, Kaohsiung, 80424, Taiwan

ARTICLE INFO

Article history:
Received 17 September 2011
Received in revised form 5 December 2011
Accepted 20 December 2011
Available online 26 December 2011

Keywords:
SAM
MEMS
IgE
FPW
Allergy bio-sensing microsystem

ABSTRACT

Utilizing self-assembled monolayer (SAM) nanotechnology, microelectromechanical systems (MEMS) and integrated circuit (IC) technologies, a flexural plate-wave (FPW) based immunoglobulin-E (IgE) bio-sensing microsystem which is capable of small test sample volume (5 μl), short operation time (<10 min), small physical size (<15 cm × 9 cm × 1 cm) and at low cost (<30 USD/test) is developed and tested. This system consists of a pair of FPW microsensors (one measurement sensor and one reference sensor) and a frequency-shift readout IC microchip. In the sensors, two 3 μm-thick aluminum (Al) reflection grating electrodes (RGE) are fabricated beside the two-port chrome/gold (Cr/Au) interdigital transducers (IDTs) to effectively reduce the high insertion loss of conventional FPW microsensors, achieved a very low insertion loss (−9.2 dB) and high mass sensitivity of human IgE antigen (-6.08×10^9 cm^2 g^{-1}) at center frequency of 6.6 MHz. A frequency-shift readout IC with high sampling resolution (31.25 kHz) has also been developed for the signal processing of the FPW biosensors. The frequency shift caused by various immobilized IgE concentrations can be accurately read out in less than 10 min which is much faster than the commercial enzyme-linked immunosorbent assay (ELISA) analysis system (>60 min).

1. Introduction

The over-reaction of immune system can cause allergies, anaphylactic shock or even fatality. In the field of immunology, mammals have five classes of immunoglobulins (IgA, IgD, IgE, IgG and IgM) corresponding to four types of hypersensitivity reactions (immediate type, antibody-dependent cytotoxic type, immune-complex disease type and delayed type). This research is focused on the testing of immediate hypersensitivity allergic reaction and the major detection target is IgE (with a molecular weight near 190 kDa) concentration in human serum. IgE molecules are present in normal human serum at extremely low concentration (less than 100 IU ml^{-1}), which is less than 1 part per million (ppm) of the total immunoglobulins in human serum [1–3]. Although there are commercial test kits based on various techniques have been reported for measuring IgE antigen concentration in human serum, including ELISA techniques [4], quartz crystal microbalance (QCM) sensing techniques [5], surface plasmon resonance (SPR) sensing techniques [6] and screen-printed electrode electrochemical sensing techniques [7]. All the above mentioned allergy test kits are with high sensitivity and precision, however, they usually require skillful complex operations, long testing time and consume large quantity of expensive chemicals.

To overcome these shortcomings, this work using MEMS and IC technologies to develop an IgE bio-sensing microsystem which is capable of small test sample volume, short operation time, small physical size and low cost. In last decade, many acoustic microsensors have been developed for molecular mass detection, such as shear horizontal surface acoustic wave (SH-SAW), surface transverse wave (STW), love wave (LW), shear horizontal acoustic plate mode (SH-APM), layered guided acoustic plate mode (LG-APM) and FPW [8–12]. However, except for the FPW device, the operating frequencies of above mentioned acoustic microsensors are usually larger than 100 MHz which will increase the difficulties of readout IC design and hindered developing low cost portable microsystem. Furthermore, since the phase velocity of the FPW device is less than the sound velocity in liquid, thus only minor energy dissipated into testing liquid, so the FPW device is more suitable for applications in clinical, industrial, environmental and biological detection compared to other acoustic microsensors [12–14]. The conventional FPW microsensor operated at low frequency (<10 MHz), could achieve high mass sensitivity (>8×10^7 cm^2 g^{-1}), but its high insertion loss (>−30 dB) usually results in a low signal to noise (S/N) ratio, and hence increasing the difficulty of signal processing [12,13]. In this research, a pair of 3 μm-thick Al RGEs are constructed beside the input and output IDTs of FPW sensor to effectively confine the launched wave energy, reduce the energy loss, and increase the

* Corresponding author. Tel.: +886 7 525200x4163; fax: +886 7 5254163.
E-mail addresses: iyuhuang@mail.nsysu.edu.tw (I.-Y. Huang), ccwang@ee.nsysu.edu (C.-C. Wang).

0925-4005/$ – see front matter © 2011 Elsevier B.V. All rights reserved.
doi:10.1016/j.snb.2011.12.065

Table 1
Physical properties of the materials adopted in this research [19–21].

	Au	Cr	Si	SiO_2	Si_3N_4	ZnO	Al
Thickness (μm)	0.15	0.02	3	0.5	0.15	1	3
Young's modulus, E (N/m^2)	7.8×10^{10}	2.8×10^{11}	1.9×10^{11}	7.0×10^{10}	3.0×10^{11}	1.3×10^{11}	7×10^{10}
Poisson's ratio, υ	0.44	0.21	0.23	0.2	0.27	0.35	0.35
Density, ρ (kg/m^3)	19 320	7194	2330	2200	3100	5606	2702
Mass per unit area, M (kg/m^2)	2.9×10^{-3}	1.4×10^{-4}	7.0×10^{-3}	1.1×10^{-3}	4.7×10^{-4}	5.6×10^{-3}	8.1×10^{-3}

S/N ratio, hence easing signal sampling and processing difficulties [15,16].

The presented allergy bio-sensing microsystem consists of a pair of FPW microsensors (one measurement sensor and one reference sensor) and a frequency-shift readout IC microchip. The frequency shift between the two FPW microsensors can be extracted and analyzed by the frequency-shift readout IC microchip. The design specifications and detailed fabrication processes of the FPW device, the quantitative analysis of the immobilized cystamine SAM/IgE antibody-antigen on the Cr/Au electrodes, the characterization of the implemented FPW-based allergy biosensor, the frequency-shift readout IC, and the IgE bio-sensing microsystem are described, respectively, in the following sections.

2. Theory and design

2.1. Theoretical analysis of the FPW device

In a FPW device, the phase velocity (V_p) of acoustic wave propagated in a very thin solid plate is much lower than that in most liquids since the thickness of thin plate is much less than the wavelength (λ), which results in very few wave energy radiation from the plate into the testing liquid [13,17]. Due to the low phase velocity, the center frequency of operation or the resonant frequency (f_0) of the FPW device for a given wavelength is low, since

$$f_0 = \frac{V_p}{\lambda} \tag{1}$$

In 1988, the phase velocity formula of a Lamb wave launched from IDTs has been proposed by Wenzel and White [18] as shown in the following equation:

$$V_P = \sqrt{\frac{1}{M}\left(T_X + \left[\frac{2\pi n}{P}\right]^2 \frac{E'}{12}d^3\right)} \tag{2}$$

Here, M, d and T_x are the mass per unit area, thickness and tension stress of the floating thin-plate, respectively. P is the period of IDTs and n is the mode number of launched wave from IDTs ($\lambda_n = P/n$). $E' = E/(1-\nu^2)$, E and ν are the Young's modulus and Poisson's ratio of silicon/silicon dioxide/silicon nitride/chrome/gold/zinc oxide ($Si/SiO_2/Si_3N_4/Cr/Au/ZnO$) floating thin-plate. In the absence of tension ($T_x = 0$) and assuming the wavelength of IDTs (four times to IDT finger width) is 80 μm, substitute the physical properties of materials listed in Table 1 [19–21] into Eq. (2), the corresponding values of E, ν, and M for a 4.82 μm-thick $Si/SiO_2/Si_3N_4/Cr/Au/ZnO$ floating thin-plate are 16.54×10^{10} N m^{-2}, 0.26, and 0.17 N m^{-2}, respectively. Hence E' is equal to 17.74×10^{10} N m^{-2} and the phase velocity (V_P) is 245 m s^{-1}. And then based on Eq. (1), the theoretical center frequency (first mode, $n = 1$) of the proposed FPW device is about 3.1 MHz.

The IDT structure is a bidirectional device and it can be converted into a unidirectional device by properly utilizing a reflector, as proposed by Zaitsev and Joshi [16]. In this paper we have adopted RGE structure as the reflector. Nakagawa and his co-worker have presented a quantitative estimation equation of the reflection coefficient (R) of a Lamb wave with a grating reflector as shown in the following equation [22]:

$$R = \tanh\ (\gamma) = \tanh\left(2\frac{\rho_m V_{Pm} - \rho_f V_{Pf}}{\rho_m V_{Pm} + \rho_f V_{Pf}}\right) \tag{3}$$

Here, the ρ_m and ρ_f are the equivalent mass densities of floating thin plates with and without RGE metal structure. The V_{Pm} and V_{Pf} are the phase velocity of Lamb wave propagated in the floating thin-plate with and without RGE metal structure. After substituted the physical properties of materials adopted in this work, listed in Table 1, the ρ_m, ρ_f, V_{Pm} and V_{Pf} can be calculated respectively as 31,717 N m^{-2}, 34,976 N m^{-2}, 371 m s^{-1} and 245 m s^{-1}. Finally, based on Eq. (3), a 30.4% reflection coefficient of the 3 μm-thick Al RGE reflector can be obtained.

Table 2
Major design specifications of the presented FPW device.

IDT finger width/gap	20 μm/20 μm
Wavelength of IDT	80 μm
Number of IDT finger pairs	25
Acoustic aperture	3.2 mm
Acoustic path length	4.38 mm
Center frequency	3.1 MHz
Number of RGE finger pairs	10
RGE finger width/pitch	20 μm/20 μm
FPW chip size	9 mm (L) × 6 mm (W)

2.2. Design of the FPW device

The major design specifications of the FPW device are listed in Table 2. The width and gap of the IDT finger electrodes are 20 μm, so that the theoretical wavelength of IDTs (four times to IDT finger width) is equal to 80 μm. Ether input or output IDTs of the FPW device is constructed by 25 pairs of Cr/Au fingers. The acoustic aperture and path length of the FPW device are designed to be 3.2 mm and 4.38 mm, respectively. In this study, two RGE microstructures are designed beside the input and output IDTs to effectively reduce the insertion loss of the FPW microsensor. Each RGE microstructure has 10 pairs of 3 μm-thick Al fingers and the width and gap of the RGE fingers are 20 μm. The total chip dimension of the presented FPW device is 9 mm (L) × 6 mm (W) × 0.415 mm (H) and its schematic layout diagram is shown in Fig. 1(a). The configuration of the proposed FPW-based allergy biosensor (with immobilized cystamine SAM/glutaraldehyde/IgE antibody/IgE antigen multilayer) is schematically displayed in Fig. 1(b).

2.3. Design of the frequency-shift readout system

The proposed frequency-shift readout system is realized using a standard 0.18 μm complementary metal-oxide semiconductor (CMOS) technology. According to the resonant basics, the output signal amplitude of the FPW allergy biosensor will be the maximum when the input frequency is equal to the central resonant frequency. Therefore, a high sensitive peak detector is needed to detect the maximum peak voltage and generate an enable signal to snapshot the corresponding frequency. By calculating the difference between the resonant frequencies of the measurement FPW

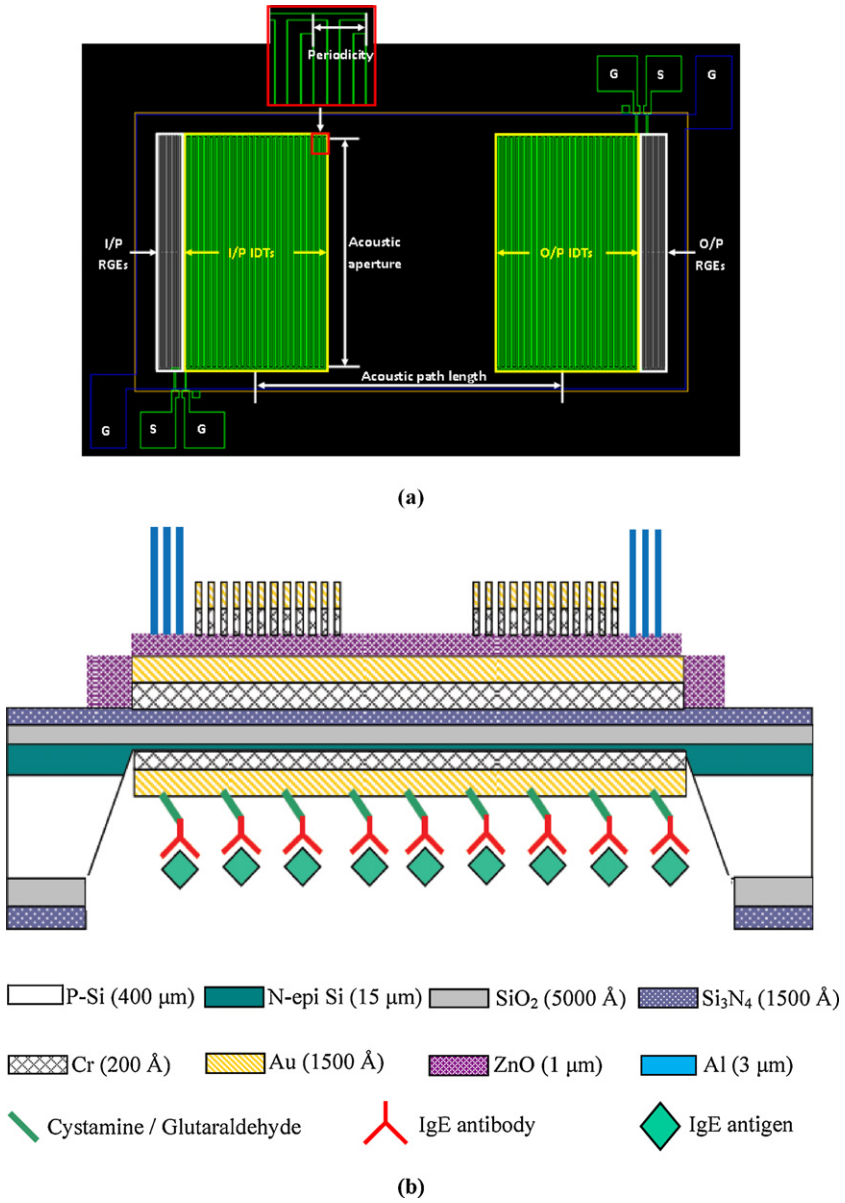

Fig. 1. (a) Layout diagram of the presented flexural plate-wave (FPW) device with two-port interdigital transducers (IDTs) and one pair of reflection grating electrode (RGE) microstructures. (b) Final configuration of the FPW-based allergy biosensor.

sensor (with IgE antigen) and reference FPW sensor (without IgE antigen), the frequency shift amount is attained such that the IgE antigen concentration can be estimated using a frequency shift versus concentration table. The proposed frequency-shift readout IC is composed of a counter, a digital-to-analog converter (DAC), an operational transconductance amplifier capacitor (OTA-C) oscillator, a pair of peak detectors, two registers, and a subtractor, as shown in Fig. 2(a). The detailed description of each subcircuit is explained in the following sections [23].

2.3.1. Linear frequency generator

Referring to Fig. 2(b), the linear frequency generator is composed of an 8-bit counter, a DAC and an oscillator; where the counter is a typical digital 8-bit counter generating 0–256 counting signal to drive the DAC. Moreover, based on the output digital code of the counter, a corresponding direct current (DC) voltage is generated to the oscillator, which is in charge of delivering a 2–10 MHz sine wave and the frequency step (resolution) is 31.25 kHz. The generated sine waves are sent to the measurement FPW and the reference FPW simultaneously.

2.3.2. Peak detector

Referring to Fig. 2(c), the peak detector in Fig. 2(a) is mainly to capture the lowest insertion loss on the FPW device in order to determine the resonant frequency. Meanwhile, the difference between the attached and unattached IgE antigen resonant frequencies are calculated, which will be converted into a binary code representation.

The measurement action procedure is as follows. Because the measurement FPW sensor of the frequency-shift readout system has attached IgE antigen causing a mass loading effect and, consequently, a shift down of the resonant frequency on the FPW device. By contrast, the resonant frequency of the reference FPW device will remain the same, since it has no IgE antigen. These two devices would then be interpreted by the respective peak detectors to find the frequency of the lowest insertion loss point, and the corresponding registers are used to capture the 8-bits

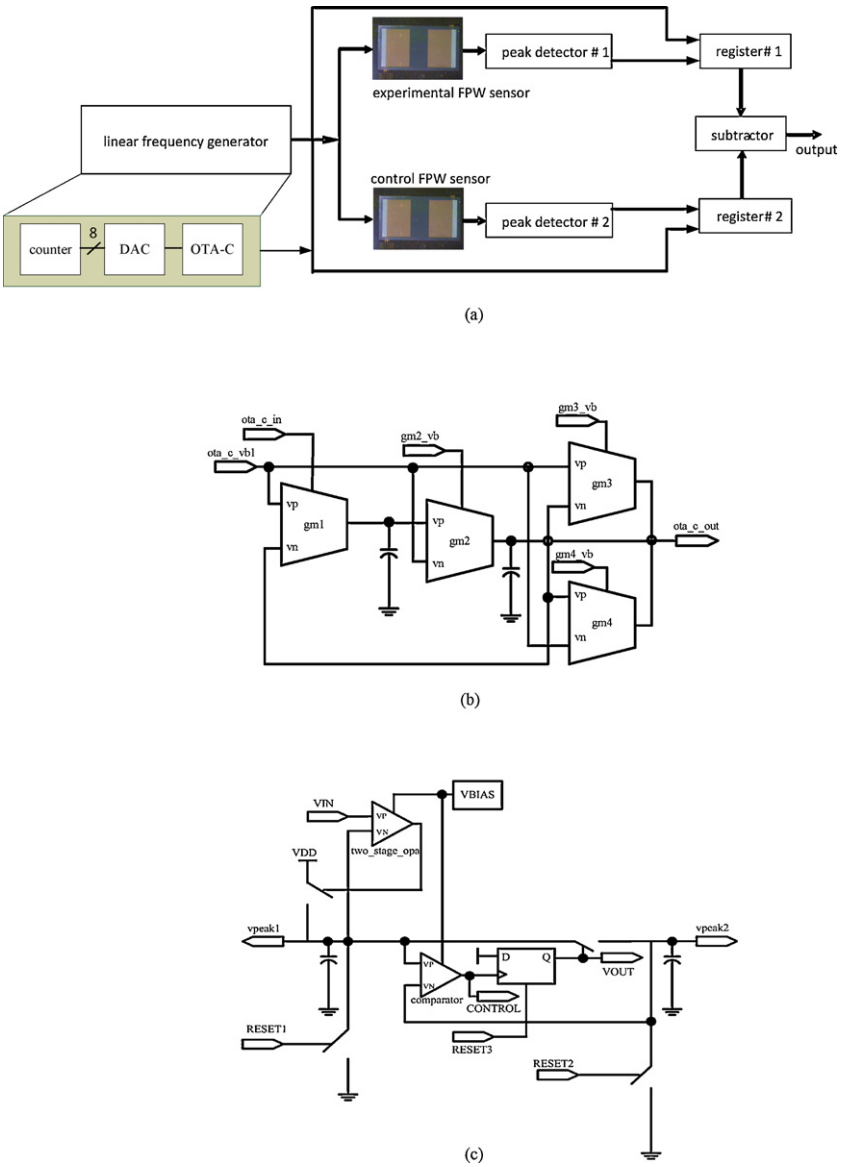

Fig. 2. (a) Schematic function block of the presented frequency-shift readout system. Schematic diagrams of (b) the linear frequency generator circuit and (c) the peak detector circuit.

digital signals from the counter. The two digital codes saved in the registers would then be calculated by the subtractor to generate a difference, which is the frequency shift corresponding to the attached IgE antigen concentration.

3. Experimental

3.1. Fabrication of the FPW device

The main fabrication processing steps of basic FPW device are shown in Fig. 3, including six thin-film material deposition/growth processes and six photolithograph processes. The materials and fabrication processes of FPW device adopted in this paper are mostly same as our previous publication [12] except for the type of wafer, backside cavity etching process and RGE microstructure. To control accurately the thickness of floating thin-plate and reduce the insertion loss of the FPW device, a 415 μm-thick 4-inch n-Epi/p silicon wafer (with a 15 μm-thick n-type epitaxial silicon layer on 400 μm-thick p-type silicon substrate), electrochemical etch-stop (ECE) process and 3 μm-thick Al RGE microstructures are adopted in this study.

The 3 μm-thick Al RGE microstructures were deposited by an E-beam evaporator and patterned by lift-off photolithographic method (photomask #4) as Fig. 3(d) shows. As shown in Fig. 3(e), after the backside SiO_2/Si_3N_4 was patterned by photomask #5 and etched with reactive ion etching (RIE) system/buffered oxide etchant (BOE), 400 μm-thick p-type silicon substrate was etched utilizing an ECE system (with 30 wt%, 90 °C potassium hydroxide (KOH) anisotropic etching solution).

In the three-electrode ECE system, a positive bias voltage of 2.55 V is applied to the n-type layer of the silicon wafer (served as working electrode, WE) by a commercial potentiostat voltage source (Autolab) via an Al ohmic electrical contact (which is patterned by photomask #6 and Al etchant). In addition, the platinum counter-electrode (CE) of the ECE system was connected to the voltage source via a current meter for detecting the etching current, and the silver chloride (AgCl) reference electrode (RE) of the ECE system is used to provide a constant voltage in the etching solution [24–26]. As the etching progressed when the reverse-biased

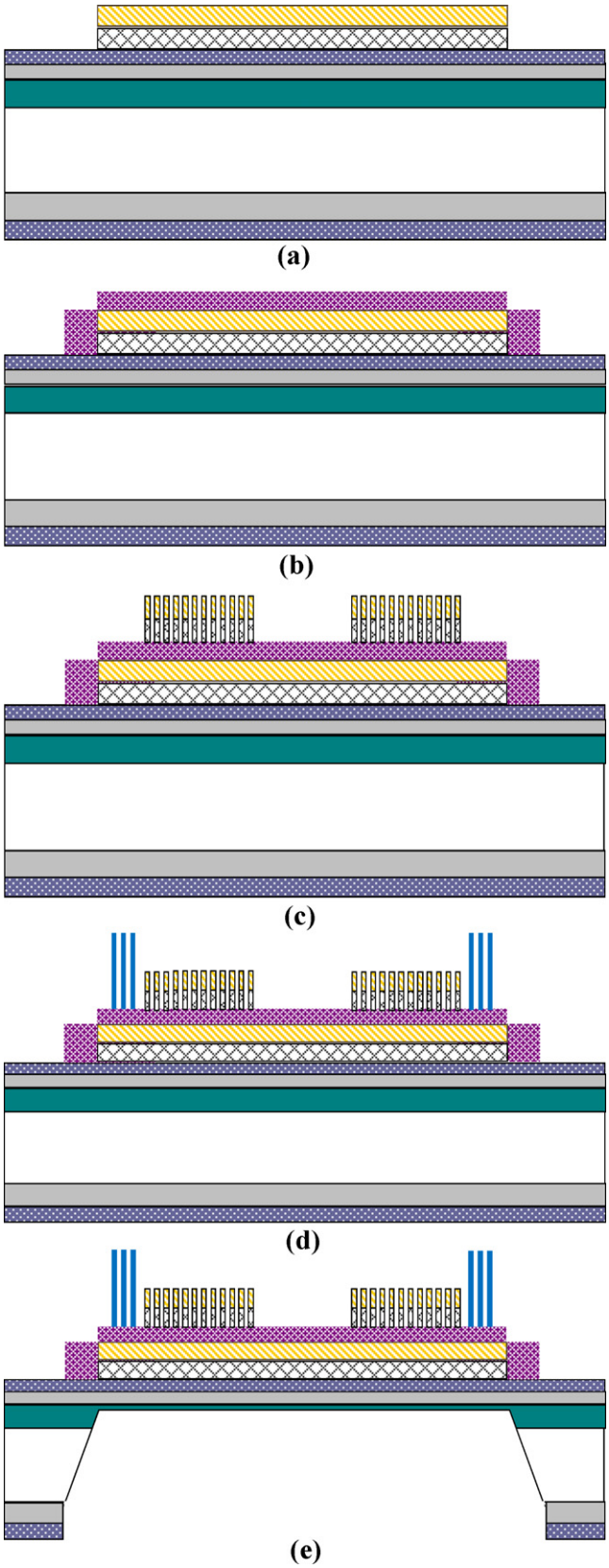

Fig. 3. Main fabrication processing steps of the FPW device.

p/n junction is reached etching will stop automatically, therefore the membrane thickness can be controlled accurately to within ±2 μm of the epi-layer thickness. Furthermore, to reduce the center frequency and increase the mass sensitivity of the FPW device, the thickness of n-type Epi-Si membrane layer was further etched to 3 μm-thick by RIE system. According to our experience, the remained 3 μm-thick thin silicon thin-plate not only can improve the electrical performance of FPW device but also provides sufficient mechanical strength and fabrication yield. Total thickness of the $Si/SiO_2/Si_3N_4/Cr/Au/ZnO$ floating thin-plate of the implemented FPW device is only 4.82 μm-thick, not including the Cr/Au IDT electrodes and Al RGE microstructures.

3.2. Immobilization of the cystamine SAM and IgE antibody-antigen layers in the backside cavity of FPW chip

3.2.1. Deposition of the Cr/Au electrode in backside cavity and packaging of the FPW chip on PCB

In general, the deposition of a SAM depends on the morphology of the underneath metal layer and Au (1 1 1) surface layer is mostly applied for the formation of SAM. As Fig. 4(a) shows, a 500 Å-thick Cr and 2500 Å-thick Au layers were continually deposited onto the backside cavity of the FPW device by an E-beam evaporator for immobilizing the SAM. To achieve a hydrophilic surface, the backside Au layer was pretreated with the 'piranha' solution (70 wt% H_2SO_4: 30 wt% H_2O_2) for 30 min, and then rinsed with deionized (DI) water three times and dried at room temperature. For improving the convenient handling of immobilization and measurement, the cleaned and dried FPW chip was adhesive die bonded, wire-bonded, and top-cover encapsulated on a printed circuit board (PCB), as shown in Fig. 4(b) and (c). The ground–signal–ground (GSG) electrodes of the FPW chip were wire-bonded to the patterned electrodes on the front side of PCB. Furthermore, the connection between PCB and the frequency-shift readout IC microchip are via universal serial bus (USB) format pins. As Fig. 4(d) shows, to avoid any damage to the floating thin-plate of the FPW chip during the immobilization process and frequency-shift measurement, a carved acrylic board was mounted on the front side of the PCB to protect the FPW chip.

3.2.2. Immobilization of the cystamine SAM/glutaraldehyde/IgE antibody/BSA/IgE antigen layers onto the backside of Cr/Au coated FPW chip

In our previous publications [9–12], a cystamine–glutaraldehyde SAM technique has been developed for the immobilization of purified mouse anti-human IgE antibody onto the backside Cr/Au electrode of the FPW microsensor. The final configuration of the proposed FPW-based allergy biosensor is shown in Fig. 1(b), detailed procedures for immobilization process are described as follows and all the procedures were performed at room temperature:

Step (1). Dip the biosensor into a 20 μl, 0.02 M cystamine solution for 1 h, washed with DI water three times and air-dried.
Step (2). Dip the biosensor into a 20 μl, 2.5 wt% aqueous glutaraldehyde reagent functioned as a cross-linking layer for 1 h and washed with DI water three times and air-dried.
Step (3). Dip the biosensor into a 20 μl diluted mouse anti-human IgE antibody for 2 h.
Step (4). Immerse the biosensor into a Tween-20 wash buffer three times.
Step (5). Immerse the biosensor into a 20 μl, 10 wt% diluted bovine serum albumin (BSA) solution functioned as a blocking layer for 0.5 h.
Step (6). Immerse the biosensor into a Tween-20 wash buffer three times.

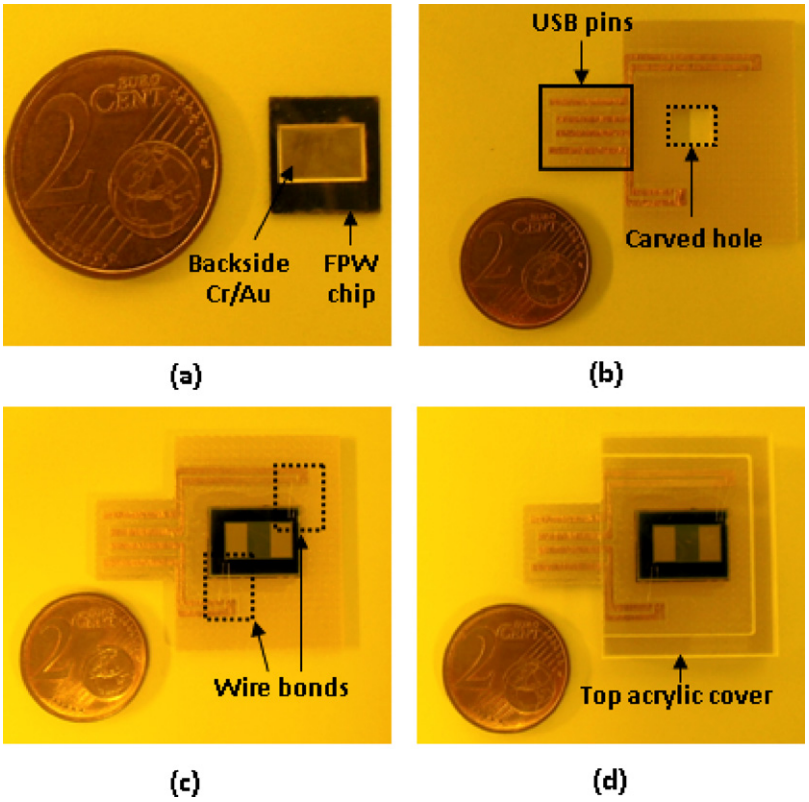

Fig. 4. (a) Backside photograph of the implemented FPW device (after backside Cr/Au deposition and patterning). Three packaging processes of the FPW device on a PCB substrate (with a central sculptured hole and USB format pins): (b) adhesive die-bonding, (b) wire-bonding and (d) top-cover (acrylic board) encapsulation.

Repeat steps (1)–(6) for testing samples under different concentrations (ranging from 38.8 to 588.8 IU ml^{-1}).

4. Results and discussion

4.1. Structure investigation of the ECE bulk micromachined FPW device

In our previous publications [9–12], a 5 μm-thick $Si/SiO_2/Si_3N_4$/Cr/Au/ZnO floating thin-plate can be realized utilizing a time-mode anisotropic KOH etching technique. However, time-mode anisotropic etching method usually resulted in a low thickness control accuracy, fabrication yield, and reproducibility. To improve the thickness accuracy of the silicon thin-plate and the fabrication yield, this work adopts an ECE technique and using n-Epi(15 μm)/p(400 μm) silicon wafer. As shown in Fig. 5(a), the initial etching current is limited by the reverse bias current of the p–n junction at around 6.3 mA before the p–n junction has been reached [23]. However, as the p–n junction is reached, a large anodic current appeared until the n-type silicon is passivated then the current falls back to the plateau value (~6.3 mA) and the etching procedure can be stopped (about 19,000 s). When the current plateau has been reached and a 15 μm-thick n-type Epi-Si layer can be left accurately, as shown in Fig. 5(b). The surface of the remained n-Epi silicon layer is very flat and the roughness on such surface is only about 40–50 nm.

4.2. Quantification analysis of the IgE antibody-antigen immobilized on 96-well microtiter plate and $Si/SiO_2/Si_3N_4$/Cr/Au/cystamine/glutaraldehyde chip

Solid-phase assays for antibody employing ligands labeled with radioisotopes or enzymes (ELISA) are probably the most widely used of all immunological assays because many samples can be performed in a relatively short time [27]. In our previous research [12], we used a commercial ELISA reader to quantitatively analyze the total IgE concentration of human serum in a microtiter plate and a high-linearity (99.37%) standard optical density (OD) curve can be extracted for six concentrations of human IgE antigen under the same monochromatized light wavelength (450 nm). In this work, we subsequently investigates the standard OD curve of the IgE antigen concentration immobilized on a $Si/SiO_2/Si_3N_4$/Cr/Au/cystamine/glutaraldehyde/IgE antibody chip with the size of 4 mm × 4 mm × 0.415 mm. As Fig. 6 shows, the standard OD curves measured on the above mentioned two substrates both presented a very high linearity (99.22–99.37%) which demonstrates the immobilization processes established on the silicon substrate is reliable for further developments on the FPW-based IgE microsensor.

4.3. Characterization of the FPW-based allergy biosensor

The center frequencies of the reference FPW device or FPW allergy biosensor were measured by the Casecade RHM-06/V probe station and the HP8714ET network analyzer. Two Cascade coplanar 150-GSG probes were used to contact the input IDTs and output IDTs of the FPW sensor and all the measurements were carried out at room temperature. As Fig. 7(a) shows, the center frequency of the reference FPW device (without coating of cystamine/glutaraldehyde/IgE antibody/IgE antigen multilayer) is about 6.6 MHz. Compared to previous research [12], this FPW device has adopted a pair of RGE microstructures to reduce dramatically the insertion loss from −50 dB to −9.2 dB. The low center frequency and low insertion loss advantages are helpful to the development of the signal processing circuit for FPW-IgE microsensors.

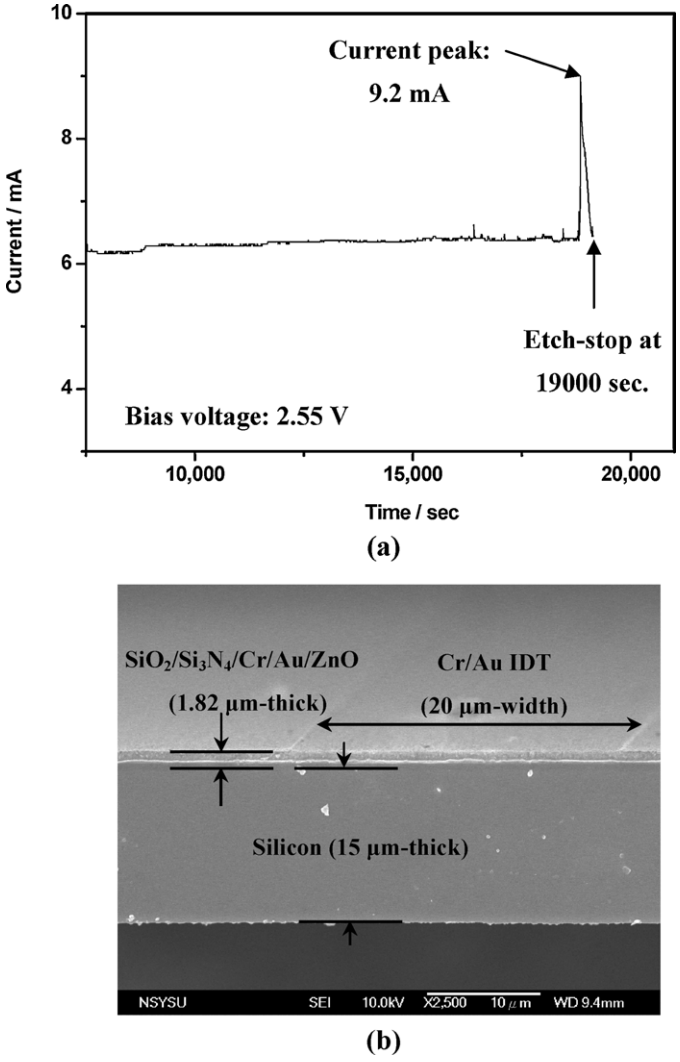

Fig. 5. (a) Detected anodic current during the electrochemical etch-stop (ECE) process of the n-Epi/p silicon wafer. (b) Cross-sectional SEM micrograph of the ECE bulk-micromachined FPW device.

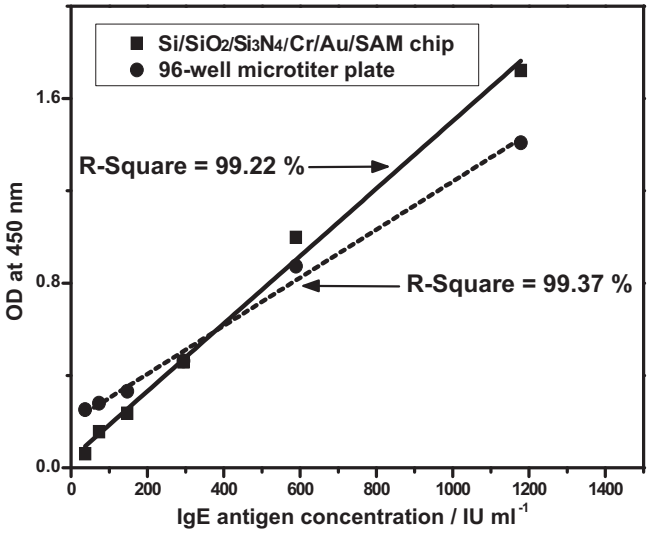

Fig. 6. The IgE standard OD curves of the (a) 96-well microtiter plate and (b) $Si/SiO_2/Si_3N_4/Cr/Au$/cystamine/glutaraldehyde chip extracted by ELISA.

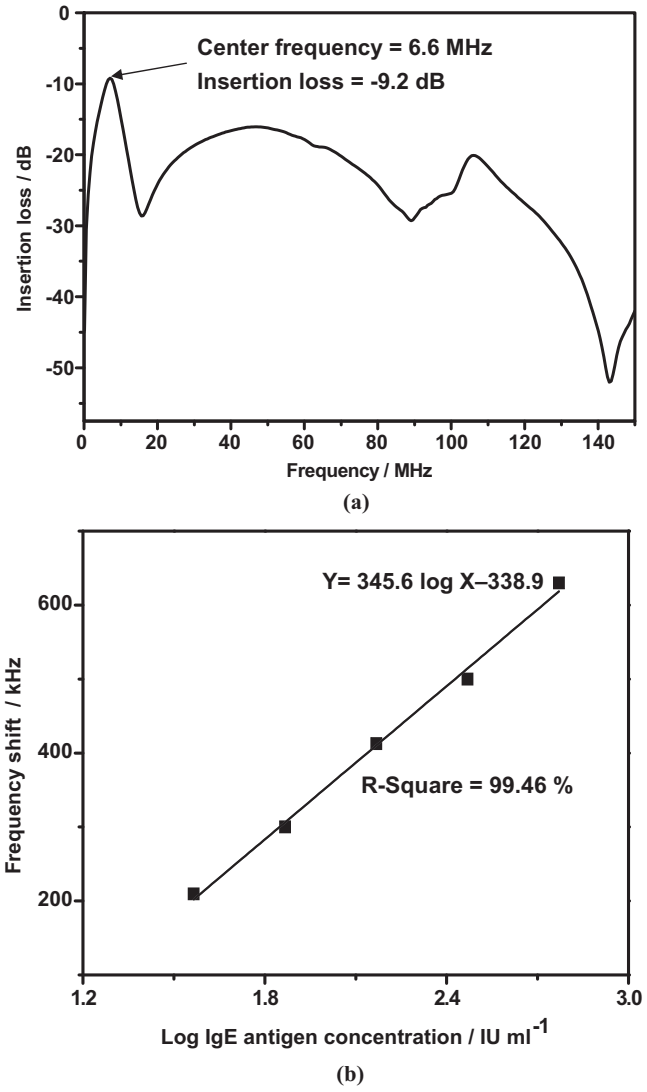

Fig. 7. (a) Frequency response of the implemented FPW device. (b) Sensing characterization of the FPW allergy biosensor under five testing with different IgE antigen concentrations.

Since the IgE antigen concentration of allergy patient is usually higher than 100 IU ml^{-1}, the FPW allergy biosensor developed in this study is coated with five different IgE antigen concentrations ranged from 38.8 to 588.8 IU ml^{-1}. As Fig. 7(b) shows, a very high sensing linearity (99.46%) of the implemented FPW allergy biosensor can be demonstrated in this research. This result is very important for developing a low-cost allergy microsystem because the non-linear compensation and correction circuits can be omitted. Based on the FPW theory [13], the calculated IgE mass-sensitivity of the FPW allergy biosensor is approximately -6.08×10^9 cm^2 g^{-1}, which is much higher than those of other acoustic biosensors.

4.4. Characterization of the frequency-shift readout IC and IgE biosensing microsystem

The frequency-shift readout die photo is shown in Fig. 8(a). The proposed readout system replaces the quantification method performed by the network analyzer with the portable circuit prototype, as shown in Fig. 8(b). By using the titration of human serum, the process of determining whether this patient has allergies

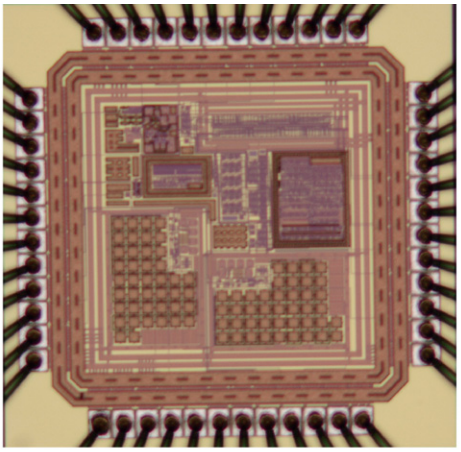

(a)

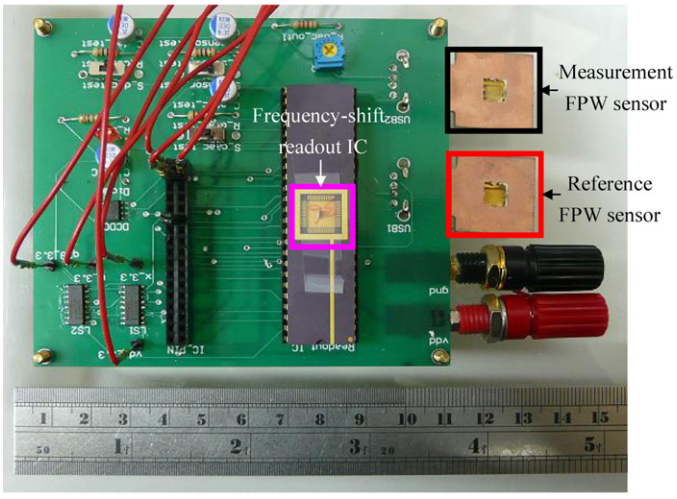

(b)

Fig. 8. (a) Die photo of the realized frequency-shift readout IC chip. (b) Photograph of the implemented frequency-shift readout system.

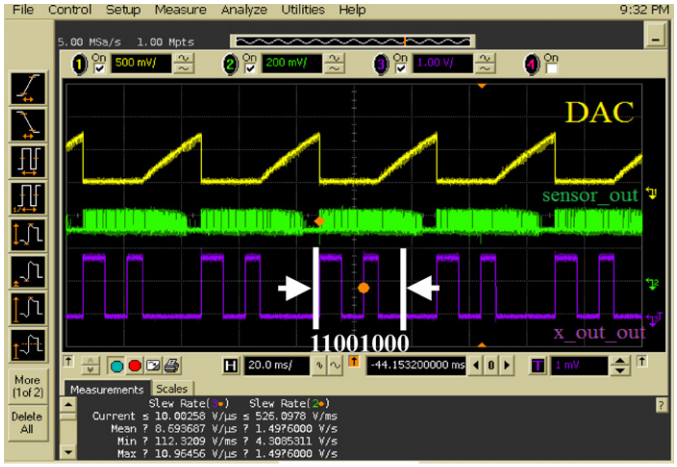

(a)

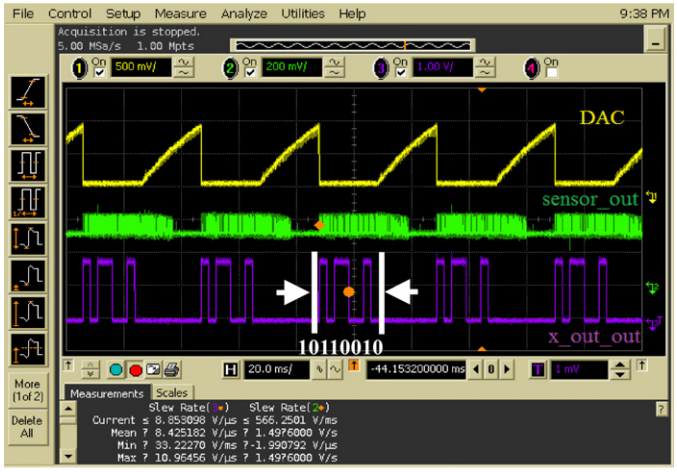

(b)

Fig. 10. Frequency response of the FPW allergy biosensor (a) before and (b) after the injecting of human serum.

can be speeded up in this research. The whole process would be accomplished in less than 10 min. Moreover, several different sub-circuits of the frequency-shift readout IC are also individually measured to justify the function correctness. Fig. 9 shows

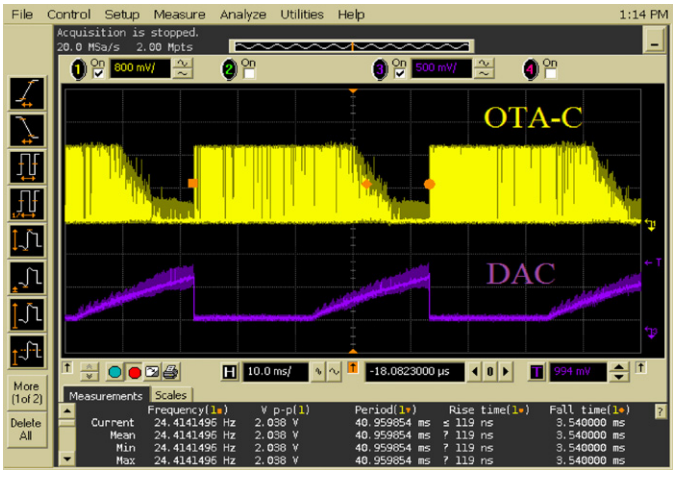

Fig. 9. Oscilloscope measurement of the OTA-C and DAC wave response.

the outputs of the DAC and the voltage to frequency converter. Fig. 10(a) shows a binary code, 11001000, before the serum is used. Fig. 10(b) demonstrates the readout digital code after serum titration, 10110010. Apparently, due to the increase of loading, the central frequency is shifted to a lower frequency appeared in the drop of the digital codes. The code difference is 00010110 indicating the frequency shift is 687.5 kHz. Based on the curve made by the concentration of IgE antigen relative to the shift of frequencies, $Y = 345.6 \log X - 338.9$, where the unit of the frequency shift, Y, is kHz, and the unit for IgE antigen concentration, X, is IU ml^{-1}; the IgE antigen concentration in the serum can thus be estimated to be 933.3 IU ml^{-1}. Whence the IgE antigen concentration in the serum is already higher than 100 IU ml^{-1}, we conclude that the patient has the traits of allergies.

Fig. 11(a) shows the transient response of the FPW allergy biosensor coated with different IgE-antigen concentrations in human serums. Notably, the frequency shift of each IgE-antigen concentration is stable after 10 min. The whole measurement time of the proposed FPW-based IgE biosensor (<10 min) is much shorter than that of the commercial ELISA analysis system (>60 min). The curve of the frequency shift versus the five different IgE-antigen concentrations is shown in Fig. 11(b), and a very high sensing linearity (99.6%) can be obtained.

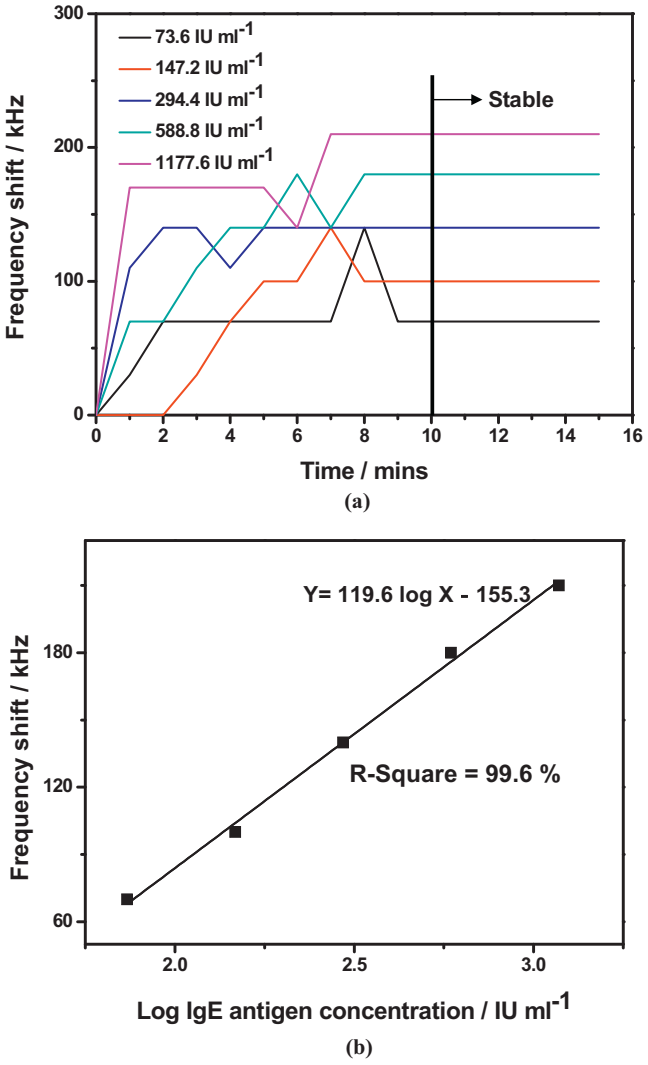

Fig. 11. (a) Timing behavior and (b) linearity characterization curves of the presented FPW allergy microsystem.

5. Conclusion

A novel human-IgE bio-sensing microsystem constructed by a pair of FPW microsensors and a frequency-shift readout IC microchip was proposed and realized in this research for allergy detection. By adding the RGE microstructures in the FPW device design and accurately control the thickness of $Si/SiO_2/Si_3N_4/Cr/Au/ZnO$ floating thin-plate, the presented FPW biosensor can achieve a very low insertion loss (−9.2 dB), low center frequency (6.6 MHz) and very high mass sensitivity of human IgE antigen (-6.08×10^9 cm^2 g^{-1}). The realized frequency-shift readout IC presents a short response time (<5 s) and high sampling resolution (31.25 kHz). The proposed allergy bio-sensing microsystem shows a 99.6% linearity and less than 10 min operation time. The developed FPW-IgE bio-sensing microsystem is capable of small sample volume (5 μl) and short operation time (<10 min), has small physical size (<15 cm × 9 cm × 1 cm) and at low cost (<30 USD/test), hence very suitable for development of an IgE point-of-care testing (POCT) microsystem.

Acknowledgments

This work was supported by Ministry of Economic Affairs and National Science Council (NSC), Taiwan, under grant 98-EC-17-A-19-S1-133, 99-EC-17-A-19-S1-133, NSC 99-2221-E-110-081-MY3 and NSC EZ-10-09-44-98. The authors are indebted to the National Nano Device Laboratories (NDL)-South Branch and the Center for Nano Science and Technology of the National Tsing Hua University (NTHU) in Taiwan for the access to their processing facilities. The authors also would like to express their gratefulness to Chip Implementation Center (CIC) of National Applied Research Laboratories, Taiwan, for their thoughtful chip fabrication service. Finally, the authors would like to thank NXP Semiconductors (Taiwan) Ltd. for their strong support of the wire bounding equipment.

References

[1] D. Male, in: I. Roitt (Ed.), Immunology, Mosby, Edinburgh, 2002, pp. 1–13 (Chapter 1).
[2] T. Platts-Mills, in: I. Roitt (Ed.), Immunology, Mosby, Edinburgh, 2002, pp. 324–341 (Chapter 21).
[3] M. Bergkvist, J. Carlsson, T. Karlsson, S. Oscarsson, TM-AFM threshold analysis of macromolecular orientation: a study of orientation of IgG and IgE on mica surfaces, J. Colloid Interf. Sci. 206 (2002) 475–481.
[4] J.E.M. Björklund, T. Karlsson, N-glycosylation influences epitope expression and receptor binding structures in human IgE, Molec. Immunol. 36 (1999) 213–221.
[5] X. Su, F.T. Chew, S.F.Y. Li, Piezoelectric quartz crystal based label-free analysis for allergy disease, Biosens. Bioelectron. 15 (2000) 629–639.
[6] X. Su, J. Zhang, Comparison of surface plasmon resonance spectroscopy and quartz crystal microbalance for human IgE quantification, Sens. Actuators B 100 (2004) 309–314.
[7] K.I. Papamichael, M.P. Kreuzer, G.G. Guilbault, Viability of allergy (IgE) detection using an alternative aptamer receptor and electrochemical means, Sens. Actuators B 121 (2007) 178–186.
[8] M.I. Rocha-Gaso, C. March-Iborra, A. Montoya-Baides, A. Arnau-Vives, Surface generated acoustic wave biosensors for the detection of pathogens: a review, Sensors 9 (2009) 5740–5769.
[9] I.-Y. Huang, M.-C. Lee, Development of a novel flexural plate wave biosensor for immunoglobulin-E detection by using SAM and MEMS technologies, in: Proceedings of the 5th IEEE Conference on Sensors (IEEE Sensors 2006), Daegu, Korea, October 22–25, 2006.
[10] I.-Y. Huang, M.-C. Lee, Y.-W. Chang, R.-S. Huang, Development and characterization of FPW based allergy biosensor, in: Proceedings of the 2007 IEEE International Symposium on Industrial Electronics (IEEE ISIE 2007), Vigo, Spain, June 4–7, 2007.
[11] I.-Y. Huang, M.-C. Lee, Development of a FPW allergy biosensor using NEMS technology, in: Proceedings of the 2008 Asia-Pacific Conference on Transducers and Micro-Nano Technology (APCOT 2008), Tainan, Taiwan, June 22–25, 2008.
[12] I.-Y. Huang, M.-C. Lee, Development of a FPW allergy biosensor for human IgE detection by MEMS and cystamine-based SAM technologies, Sens. Actuators B 132 (2008) 340–348.
[13] D.S. Ballantine Jr., R.M. White, S.J. Martin, A.J. Ricco, G.C. Frye, E.T. Zellers, H. Wohltjec, Acoustic Wave Sensors: Theory, Design, and Physicochemical Application, Academic Press, New York, 1997.
[14] J. Bjurstrom, V. Yantchev, I. Katardjiev, Thin film Lamb wave resonant structures – the first approach, Solid State Electron. 50 (2006) 322–326.
[15] S.G. Joshi, B.D. Zaitsev, I.E. Kuznctsova, Reflection of plate acoustic waves produced by a periodic array of mechanical load strips or grooves, IEEE Trans. Ultrasound Ferroelectr. Freq. Control 49 (2002) 1730–1734.
[16] B.D. Zaitsev, S.G. Joshi, Reflection of ultrasonic Lamb waves produced by thin conducting strips, IEEE Trans. Ultrasound Ferroelectr. Freq. Control 46 (1999) 1539–1544.
[17] P. Luginbuhl, S.D. Collins, G.A. Racine, M.A. Grétillat, N.F. de Rooij, K.G. Brooks, N. Setter, Microfabricated Lamb wave device based on PZT sol–gel thin film for mechanical transport of solid particles and liquids, IEEE/ASME, J. Microelectromech. Syst. 6 (4) (1997) 337–346.
[18] S.W. Wenzel, R.M. White, A multisensor employing an ultrasonic Lamb-wave oscillator, IEEE Trans. Electron Devices 35 (1988) 735–743.
[19] J.W. Gardner, V.K. Varadan, O.O. Awadelkarim, Microsensors MEMS and Smart Devices, John Wiley & Sons Inc, New York, 2001 (Appendix F).
[20] J.K. Chen, K.L. Tang, J.T. Chang, Effects of zinc oxide on thermal shock behavior of zinc sulfide–silicon dioxide ceramics, Ceram. Int. 35 (2009) 2999–3004.
[21] T.R. Hsu, MEMS and Microsystems: Design and Manufacture, McGraw-Hill, Boston, 2005, pp. 250–251.
[22] Y. Nakagawa, M. Momose, S. Kakio, Characteristics of reflection of resonators using Lamb wave on at-cut quartz, Jpn. J. Appl. Phys. 43 (2004) 3020–3023.
[23] C.-H. Hsu, Y.-R. Lin, Y.-D. Tsai, Y.-C. Chen, C.-C. Wang, A frequency-shift readout system for FPW allergy biosensor, in: 2011 IEEE International Conference on IC Design and Technology (ICICDT 2011), Kaohsiung, Taiwan, May 2–4, 2011.
[24] L. Wallman, J. Bengtsson, N. Danielsen, T. Laurell, Electrochemical etch-stop technique for silicon membranes with p- and n-type regions and its application to neural sieve electrodes, J. Micromech. Microeng. 12 (2002) 265–270.
[25] S.S. Wang, V.M. Mchneil, M.A. Schmidt, An etch-stop utilizing selective etching of n-type silicon by pulsed potential anodization, J. Microelectromech. Syst. 1 (1992) 187–192.

[26] M.J. Madou, Fundamentals of Microfabrication: the Science of Miniaturization, 2nd ed., CRC Press, Boca Raton, FL, 2002, pp. 235–236 (Chapter 4).
[27] M. Steward, in: I. Roitt (Ed.), Immunology, Mosby, Edinburgh, 2002, pp. 417–433 (Chapter 27).

Biographies

I-Yu Huang was born in Taiwan in 1967. He received M.S. and Ph.D. degrees in the Department of Electrical Engineering from National Tsing Hua University (NTHU), Taiwan. His doctoral dissertation was entitled "A monolithic high performance ISFET pH-sensor with integrated miniaturized solid-state reference electrode. During 2001–2002, he joined the Asia Pacific Microsystems Inc. and contributed to build up a MEMS mass-production line and the process integration of MEMS-related products. Since 2003, he has devoted his professional career to the Department of Electrical Engineering, National Sun Yat-Sen University (NSYSU), as an assistant professor. On February 1, 2009, he became an Associate Professor of NSYSU and his recent researches focus on the development of biomedical and electrochemical microsensors, electrostatic-drive microactuators and RF-MEMS. He has been a member of the Institute of Electrical and Electronics Engineers (IEEE) since 2004. He has been Director of Operation Center of Industry and University Cooperation, NSYSU, Taiwan, since August 2010.

Ming-Chih Lee received the B.S. degree in electronic engineering from St. John University in 2003 and the M.S. degree in electrical engineering from Da Yeh University in 2005, Taiwan. Currently, he is working toward the Ph.D. degree in the electrical engineering department of NSYSU, specializing in biosensors development.

Chia-Hao Hsu was born in Taiwan in 1981. He received the B.S. and M.S. degree in electronic engineering from Southern Taiwan University in 2005 and 2007, respectively. He is currently working toward the Ph.D. in the Department of Electrical Engineering of NSYSU, Taiwan. He recent research interests include VLSI design and mixed signal integrated circuit design.

Chua-Chin Wang was born in Taiwan in 1962. He received the B.S. degree in electrical engineering from National Taiwan University in 1984, and the M.S. and Ph.D. degree in electrical engineering from State University of New York in Stony Brook in 1988 and 1992, respectively. He then joined the Department of Electrical Engineering, National Sun Yat-Sen University (NSYSU), Taiwan. His recent research interests include mixed-signal circuit design, low-power and high-speed circuit design, communication interfacing circuitry, and bio-chips. He was the Director of Engineering Technology Research & Promotion Center (ETRPC), NSYSU, between 2007 and 2009. He has been Chairman of Department of Electrical Engineering, NSYSU, Taiwan, since 2009. Dr. Wang was General Chair of 2007 VLSI Design/CAD Symposium. He was Chair of IEEE Circuits and Systems Society (CASS), Tainan Chapter, from 2007 to 2008. He was also Chair of IEEE Solid-State Circuits Society (SSCS), Tainan Chapter, from 2007 to 2008. He was the founding Councilor of IEEE NSYSU Student Branch in 2007. He is also a member of the IEEE CASS Multimedia Systems & Applications (MSA), VLSI Systems and Applications (VSA), Nanoelectronics and Giga-scale Systems (NG), and Biomedical Circuits and Systems (BioCAS) Technical Committees. He is a senior member of IEEE since 2004. He was a Guest Editor of *International Journal of Electrical Engineering*, and *Journal of Signal Processing Systems*. Currently, he is also serving as the Associate Editor of International *Journal of VLSI Design*, IEICE *Transactions on Electronics*, and *Journal of Signal Processing Systems*. He is IEEE CASS Nanoelectronics and Giga-scale Systems (NG) Technical Committee Chair term from 2008 to 2009.